Invited paper presented at the
1979 Nuclear Science Symposium,
17-19 October 1979, Sheraton Palace
Hotel, San Francisco. To be published
in IEEE Trans. Nuc. Sci.

BNL 26850

CONF-791037--19

FAST NEUTRON DAMAGE IN GERMANIUM DETECTORS*

H. W. Kraner

Brookhaven National Laboratory
Upton, New York 11973

October 1979

*This research was supported by the U. S. Department of Energy:
Contract No. EY-76-C-02-0016.

Invited paper presented at the
1979 Nuclear Science Symposium,
17-19 October 1979, Sheraton Palace
Hotel, San Francisco. To be published
in IEEE Trans. Nuc. Sci.

BNL 26850

FAST NEUTRON DAMAGE IN GERMANIUM DETECTORS*

H. W. Kraner

Brookhaven National Laboratory
Upton, New York 11973

October 1979

*This research was supported by the U. S. Department of Energy:
Contract No. EY-76-C-02-0016.

FAST NEUTRON DAMAGE IN GERMANIUM DETECTORS*

H. W. Kraner

Brookhaven National Laboratory
Upton, New York 11973

ABSTRACT

The effects of fast neutron radiation damage on the performance of both Ge(Li) and Ge(HP) detectors have been studied during the past decade and will be summarized. A review of the interaction processes leading to the defect structures causing trapping will be made. The neutron energy dependence of observable damage effects will be considered in terms of interaction and defect production cross sections.

1. Introduction

One of the first areas of application for Ge(Li) spectrometers in the mid 1960's was in the gamma spectrometry involved with light ion nuclear reaction physics at low energy accelerators. Many studies in this area produced substantial fast neutron backgrounds, and it was soon and sadly discovered that the precious Ge(Li) detector was very soon adversely affected. The highly prized energy resolution was observed to greatly worsen over the course of an experiment. Several early empirical studies[1-3] established the working levels for this problem. It was found that devices that were damaged could be repaired by various annealing recipes, and the problem of damage did not prevent the use of Ge(Li) detectors in potential damaging environments. Thus, germanium detectors continued to be used, damaged, and repaired with little more than empirical understanding and evaluation of the damage processes that had occurred.

The advent of high purity germanium in the early 1970's added another dimension to the potentiality for study of fast neutron damage in germanium, and several empirical studies were conducted on the damage processes in this material. Damage tolerances and effects were found not to be vastly different from Ge(Li) detectors, but the effects of temperature cycling (annealing) and changes in bulk conductivity could be studied conveniently and without the possibility that the interstitial Li ion played a role in damage or recovery.

Curiously, as some renewed interest in the problem of fast neutron damage has occurred,[4,5] the incidence of damage to germanium detectors from many processes in nuclear physics research has dwindled as evidenced by fewer detectors being returned to manufacturers for repair.[6] Along with perhaps less activity in light-ion physics, more germanium detectors are currently used in essentially nonexperimental, monitoring applications. However, even though the immediate need for improved repair capability (for example) from better basic understanding of the damage effects is somewhat lessened, the general problem of understanding the effects of fast neutron damage in germanium detectors remains and is inherently challenging.

As the problems of fast neutron damage were just being recognized, the general field of radiation damage in semiconductors was in a period of growth with frequent conferences and published proceedings.[7] These contributions had little impact on the particular problem of germanium detectors for several reasons including the reluctance of the detector community to reach into the general damage literature. However, several other factors can be mentioned: (i) many studies were made with germanium at room temperature which is a very different problem from that of present concern, (ii) damage studies had tended to be carried out at much greater fluences than those found to affect germanium detectors, and (iii) many studies and research programs were directed around electron or gamma ray induced damage which produces isolated defects in contrast to the effects of fast neutron damage. (Even as the effects of ion implantation--which better approximate fast neutron damage--are now being studied, the fluences involved are far from being comparable.) Also, it can be remarked that, as always, considerably more effort has gone into silicon than germanium. Germanium detectors are extremely sensitive indicators of electronic effects of damage, and the very low fluences ($\sim 10^{10}$ n/cm^2) encountered are seldom of interest in the general damage literature.

2. The Experimental Background

The first purposeful study of fast neutron damage in germanium spectrometers was carried out by Kraner, Chasman, and Jones[2] in which several small planar Ge(Li) detectors were exposed to 1.1, 5.75, and 16.5 MeV monoenergetic neutrons. Degraded energy resolutions were observed between 1 and 2 x 10^{10} n/cm^2, and hole trapping was established as the cause. By way of introduction, Fig. (1) is the sort of effect on energy resolution that is to be expected. Figure (2) shows the preponderance of hole trapping in the detector irradiated at 5.75 MeV when ^{60}Co γ rays are collimated onto the edge near the n+ contact (hole traversal) compared to the edge near the contact (electron traversal). In addition, the spectra are sorted two-dimensionally with the far axis (y) being increasing pulse rise time which further delineates events in which carriers had to make a full traversal of the detector. It is clear that the case in which holes make the full detector traversal shows the greatest trapping. Although only several detectors were irradiated, the order of damage was found to be that the detector irradiated with 16.5 MeV neutrons showed resolution degradation at the least fluence, followed by the 5.75 MeV and 1.1 MeV detectors although the fluence range of obvious damage was less than a factor of three for these detectors. Due to the early stage of development (5 keV resolution), direct comparisons with the several later studies should not be made. The resolution effect could be explained by isolated defects having $\sim 10^{-15}$ cm^2 cross sections and was also compatible with defect cluster cross sections. Complete recovery was achieved after a standard "cleanup" drift.

Stelson et al.[8] found a much lower fluence of $\lesssim 10^9$ n/cm^2 adversely affected a coaxial Ge(Li) which may be expected if hole trapping predominates for a detector geometry that requires holes to largely originate in a low field region and make a full volume traversal.

As mentioned in the introduction, high purity germanium detectors offered several distinct advantages towards the study of radiation damage: they can be annealed or temperature cycled without detriment to the

*This research was supported by the U. S. Department of Energy: Contract No. EY-76-C-02-0016.

detector requirements, and they are relatively pure and uncompensated as a material in which interstitial lithium can not play a role in the damage or annealing. An early study by Llacer and Kraner[9] on small high purity planar detectors irradiated mainly at 1.6 MeV verified that obvious damage occurred at fluences between 1 and 3 x 10^{10} n/cm^2. The effect of a 20° C anneal following this final irradiation step was found to produce an exaggerated effect on the energy resolution, and that complete recovery was achieved with a 250° C anneal. Moreover this study included both n and p-type Hall effect measurements on irradiated Hall samples to define defect levels. The damage-annealing cycle was found to eliminate some deep acceptor levels in the original p-type material. A Ge(Li) detector was directly compared, and no great difference in damage susceptability was found. Some decrease in the number of preirradiation acceptor levels was observed following irradiation and also annealing in p-type material. This is consistent with the general damage literature in which n-type material converts to p-type, and p-type material improves.

Goulding and Pehl[3] described their experience with neutron damage of Ge(Li) and Si(Li) detectors and summarized the neutron damage studies through 1971. They were able to temperature cycle several Ge(Li) detectors for brief periods at 25° C and observed the enhanced resolution degradation on return to 77° K that had been seen with high purity detectors. Hole trapping was affirmed, and complete restoration was achieved following a ~00° C rediffusion and redrift.

Kraner, Pehl, and Haller[10] attempted a more comprehensive study of fast neutron damage in planar high purity germanium detectors but included several Ge(Li) detectors for direct comparison. Most detectors were irradiated with 5.5 MeV neutrons, but one was exposed to 1.4 MeV neutrons and one to 16.4 MeV neutrons. Several results from this study are listed:

(a) The range of detectable "damage thresholds" varied for the several detectors by perhaps as much as a factor of 5 indicating a possible unknown material dependence to damage hardness.

(b) Thermal cycling, an attractive feature of high purity germanium detectors, to even 200° K greatly enhanced the damage already present in the device and should be avoided in routine use.

(c) As the irradiation proceeded in sequential fluence steps, the base (undepleted) material resistivity was found to increase significantly so that the device capacitance was forced to the geometrical value with no C(V) variation.

Figure (3) shows the several C(V) characteristic of detector 1094-4 during the course of the neutron irradiation. The capacity was measured by inserting a pulser whose voltage was calibrated against a source to give a known charge on the preamplifier input in a dc-coupled system.[11] At biases below depletion, the resistivity of the undepleted base material is usually so low that the base material capacity is shorted and does not appear in series with the depletion depth capacity. (In some high purity material, the base resistivity may not be completely negligible.) If damage forces the material resistivity to rise, the undepleted region appears as an RC parallel circuit in series with the depletion capacitance; the RC effect is shown in Fig. (4) as a greatly slowed component of the rise time on the pulser pulse. The initial pulse feedthrough by the geometric capacitance portion of the impedance is evident. The resistivity of the base material was derived from this shape to be ~ 100 KΩ-cm whereas it was estimated to be ~ 1 KΩ-cm initially at 80° K. This effect could be useful in monitoring the accumulated damage in a detector in use.

(d) Very complete annealing of the observed energy resolution degradation can be accomplished at temperatures of about 100° C which leads to the tempting possibility of in situ annealing.

(e) If detectors which supported relatively high fields are compared for damage responses to 1.4, 5.5, and 16.4 MeV neutrons, a difference as a function of fluence of perhaps a factor of five is found, suggesting some dependence of energy resolution degradation on the neutron energy spectrum.

Pehl, Varnell, and Metzger[12] exposed two planar high purity germanium detectors to 6 GeV/c protons and found a much lower fluence limit for damage than with neutrons, specifically ~ 2 x 10^8 p/cm^2. A very sharp "annealing" stage was found at 120° K after which the energy resolution was greatly worsened after returning to operation at 80° K. The broadened line shapes were found to be dissimilar to those found in neutron damage indicating possibly some influence of electron (as well as hole) trapping.

Pehl, Madden, Elliott, Raudorf, Trammell, and Darken[13] compared the neutron damage "hardness" or tolerance of two high purity coaxial detectors which were constructed with opposite n^+ p^+ electrode structures. A detector having the conventional outer peripheral contact as n^+ forces the holes to originate and travel a generally larger distance to the inner p^+ contact than one with the outer electrode being p^+ and the inner n^+. As expected, the configuration with the outer p^+ contact permitted the very trap sensitive holes to be directly collected and was found to maintain workable energy resolution (e.g. 3 keV) to fluences greater by a factor of ~ 30 than the inverse configuration. These effects are shown in Fig. (5). This factor was to some extent predicted[14-16] and fulfills early predictions that the effects of hole trapping can be minimized.

In this same vein, Martini[17] has noted that high purity coaxial detectors made from portions of ingots which are found to trap holes and which have regions that are n-type (as well as portions which are p-type) produce acceptable energy resolution when made in the outer p^+, n-type configuration. The p-type portions of the ingot which are structured in the usual outer n^+ electrode configuration show obvious hole trapping and result in ≳ 3 keV ^{60}Co resolutions whereas the n-type portions with the outer p^+ electrode give detectors with commercially acceptable 1.85 keV ^{60}Co gamma ray resolutions.

Planar detectors made from several high purity germanium ingots having vastly different chemical impurities were irradiated by Hubbard and Haller.[5] The fluence of PuBe neutrons required to degrade energy resolution to 3 keV was found to be ~ 3 x 10^{10} n/cm^2 for small planar detectors made from ingots having individually substantial concentrations of H_2, O_2, and Si. Careful attention was given to measuring the detector response at identical internal fields (1000 V/cm being optimum) which may have been an important factor in the "threshold" fluence variability of the

several detectors not fully appreciated or considered in earlier work.[10]

Darken et al.[4] have produced the most comprehensive consideration of the electrical nature of fast neutron induced defects to this date. In order to explain the resolution transients observed after the irradiation of the p and n-type coaxial detectors described by Pehl et al. a complete analysis of the charge states of both disordered regions and isolated defects was undertaken. These resolution transients have also been considered in detail by Hubbard and Haller[5]. The case for both large disordered regions and isolated defects (which are also possible and probable) for fast neutron damage was considered with the conclusion that each may play a role. Figure (6) shows the effect that forced a more thorough investigation of the charge states of damage induced defects. After the irradiation to 7×10^9 n/cm^2 unmoderated 252 Cf described in Ref. 13 the p-type coax, P382, reached a resolution of $\sim$ 44 keV. The n-type detector, N328, was only degraded to $\sim$ 4 keV following 1×10^{10} n/cm^2 at the same source. The bias was switched off for a period and returned to each detector. P382 was found to directly improve to $\sim$ 4 keV and proceeded to degrade back to the steady state value of $\sim$ 44 keV. The n-type coax improved from 17 keV to its post irradiation value over the same period. The source itself was found to play a role in providing holes to neutralize the trapping centers of the n-type detector as the transient improvement was very slightly noticed over 16 hours without the source being present and greatly speeded by a source at close range. No source effect was noted in the transient effect of the p-type detector. The improvement of the n-type coax can be directly interpreted by the neutralization of the charge on the large disordered regions which would be expected to remain charged (p-type) within the n-type matrix without bias in the undepleted material. Consideration of the hole current densities and cross section yields a calculated time constant of 35 min compared with $\sim$ 70 min observed which may be considered good agreement. The hole trapping cross section must, however, be reduced by about an order of magnitude to $\sim 10^{-10}$ cm^2 or somewhat less. The transient in the p-type coax must be explained by the effective hole trap becoming neutralized in the undepleted zero bias condition (a p-type defect in p-type material) and having a sufficiently large detrapping probability to achieve a negatively charged equilibrium condition after biasing, when the majority carriers are not available for neutralization. An explanation in terms of isolated defects (as opposed to disordered regions) is given for an isolated defect with a trap depth of E_v + .27 ev, which gives a 70 min exponential transient response (and is not far from a E_v + .31 ev acceptor observed by Konopleva[18]).

Darken suggests that the disordered region from a 1 MeV neutron in n-type Ge may acquire $\sim$ 100 (net) charges when unbiased. The hole trapping cross section is determined by the electrostatics of this embedded charge and is given by

$$\sigma_{geom.} = \pi r_f^2 = \frac{Q}{E\varepsilon} \qquad (1)$$

where r_f is a radius from the disordered region to which the field lines are distorted little enough to not affect a moving hole, Q is the accumulated charge, E the detector field, and ε the dielectric constant. This expression can be derived by considering the forces on a charge moving in the field E past a fixed charge Q. If E is 2 kV/cm, r_f is $\sim 4 \times 10^{-3}$ cm giving a cross section of $\sim 6 \times 10^{-9}$ cm^2 which is much larger than the disordered region itself and rather greater than that required to produce the $\frac{\Delta E}{E} = \frac{\Delta Q}{Q} = 10^{-2}$ effect commonly observed for resolution degradation. As noted, the interpretation of the transient response requires a somewhat smaller cross section. This "size" of disordered region is, however, large enough to explain the reduced conductivity of the undepleted region which causes the lessened voltage dependence of the device C(V) function, especially considering its possible 1/E field dependence. This study most convincingly poses the question whether observable neutron damage is caused by isolated defects or the charge on large disordered regions; it may be both. Transient effects similar to those from the p-type coax have been observed but not studied in detail in damaged Ge(Li) coaxial detectors.[19]

Before summarizing the observations of fast neutron damage in germanium detectors, it may be helpful to consider several contributions from the literature on damage particularly as they pertain to an understanding of annealing. The concept of large disordered regions produced by affective short ranged recoils from fast neutrons is well established and was very early appreciated by Crawford and Cleland[20] and Gossick[21] who modeled the long-ranged effect. Their consideration of the disordered regions effect on carrier mobility based on a volume fraction (f) rather than extended, field dependent cross section may not be applicable to the high purity GE low fluence situation of immediate interest. The existence of the large disordered regions is undisputed, having been seen by electron microscopy[22] and very directly inferred by several other effects including material length changes[23-25]. Figure (7) is reproduced from Bertolotti[26] to show neutron produced disordered regions in n-type germanium which have extents of $\sim$ 150 - 200 Å (somewhat affected by the etch rate used to delineate the region).

Konopleva et al.[18] have studied the several annealing stages of both n and p-type germanium irradiated at 77° K by fast (reactor) neutrons up to fluences of 5×10^{15} n/cm^2. Annealing stages between 77° and 500° K were carried out with both n and p-type samples in the range of 1-10 Ωcm. Of direct interest is the fact that the conductivity of the p-type sample decreased markedly from $\sim$ 1 ohm^{-1} cm^{-1} to perhaps 1/100 of that value during anneal from 77° K to 150° K (defect "ripening") and then returns to its original high value abruptly slightly above 200° K. The carrier concentration does not show this stage so dramatically nor does the n-type conductivity. (It is noted, however, that the carrier concentration measurements are perhaps suspect due to the high γ background during the measurements.) Also, the value to which this p-type conductivity decreased is perhaps simply near the original value for high purity germanium. Further work by this author has described conductivity in the presence of large disordered regions as having a "percolation" character.[27] Extensive photoconductivity data were taken showing that many defect levels--both donors and acceptors--were annealed in the 77° - 150° K ripening stage and that the Fermi level shifts to the center of the gap. Donors tended to anneal between 150° and 230° K, resulting in the loss of two levels, E_v + 26 eV and E_v + .34 eV, with the remaining levels of E_v + .18, E_v + .31, E_c - .32, and E_c - .25 eV being all acceptor levels. These residual levels are not unlike the more stable defect levels observed in room temperature irradiations. Complete annealing was accomplished by the 500° K cycle. The authors attribute the defect ripening stage as a lattice "rearrangement" around the vacancy, interstitial rich cluster. Unfortunately, few details of the microstructure of the defect cluster were inferred from these measurements. It would be of interest to know if the

defect "ripening" stage could proceed with time (as opposed to temperature) and/or might be bias aided so that it could effectively occur during neutron damage at ~ 80° K. Some vacancy motion is certainly expected, and this "arrangement" would occur in and around the defect cluster. The early annealing of donors between 150° and 230° K may or may not have some bearing on the suggested break up of large clusters[24] into several smaller ones but does leave the material with only active acceptors, consistent with most models. The "fragile" donors can also arise from isolated defects which disappear into many sinks following the 10^{13} n/cm² irradiation, a relatively high fluence. Some contributions to the dynamics of cluster formation and annealing have been considered more recently by Martynenko[28,29]

An interesting and dramatic experiment on vacancy migration has been published by Whan[30,31] on infrared absorption studies of oxygen doped, n-type germanium. This experiment is reported here as it is graphic evidence on the motion of vacancies from neutron damage at low temperature and gives an indication of the break up of cluster type damage. A 620 cm^{-1} absorption band is established to be due to a vacancy oxygen complex; its presence can be an indicator of the motion or activity of vacancies seeking oxygen following, or during, irradiation. Figure (8) shows this band as it develops following ~50° C irradiation and annealing. Figure (9) follows the band concentration for both fast neutron and electron radiation from the low temperature irradiation through anneals at increasing temperatures. Following 4×10^{14} n/cm² at ~50° C (220° K), there is little intensity in the 620 cm^{-1} band shown in Fig. (8). The clustered damage regions are sufficiently stable to not anneal at that temperature (the vacancy must move to find an interstitial oxygen). Comparing the intensities of the 620 cm^{-1} band in Fig. (9), the electron irradiations are dramatically different showing the 620 cm^{-1} band at temperatures as low as 100° K. The isolated vacancies are not captive in a cluster, are evenly distributed throughout the sample, and have sufficient mobility to find and form the oxygen complex. However, as the samples are annealed starting from just below room temperature the 620 cm^{-1} grows in the neutron irradiated samples as the clusters apparently break up and release individual vacancies. At temperatures above 100° C the 620 cm^{-1} band diminishes in both the neutron and electron irradiated samples, and other more stable complexes grow in. Whan also notes the results of Vook[24] on length changes in deuteron irradiated germanium, the annealing of which above 200° K was interpreted as the breaking up of clusters into smaller ones.

One is thus led to believe that the defects formed in Ge detectors at 77° K are sufficiently stable to remain as localized clusters of vacancy interstitial pairs. A definite annealing "stage" occurs between 120 and 200° K [27,24], and the cluster begins to break up at temperatures above 220° K.

3. Summary of Observations

(1) The energy resolution of germanium spectrometers, both Ge(HP) and Ge(Li), operated at ~ 80° K, is noticeably degraded by fluences of fast neutrons of between 10^9 and 10^{10} n/cm².

(2) Fast neutron damage causes predominant hole trapping which is associated with the well-known disordered regions having dimensions of several hundred angstroms. The fixed charge on these disordered regions may be as much as 100 e, may vary depending on the bias history, and play a significant role in the trap efficiency on cross sections. Thus resolution transients following bias cycling have been observed and explained. Coaxial detectors of n-type Ge with the outer peripheral contact configured as p⁺ require the holes to move least and offer greatly improved damage hardness.

(3) The role of isolated defects--or perhaps smaller disordered regions or clusters--is not as yet clear although they may be origins for hole trapping, also. This type of damage may have more bearing on high energy proton induced damage.

(4) The rise in base material resistivity during damage which obscures the capacitance vs. voltage measurement can be explained by the reduced carrier mobility of the undepleted region caused by the very extensive space charge of charged, disordered regions.

(5) An apparent material dependence of radiation damage tolerance may have been due to some variability in the applied field of the several devices studied.

(6) The annealing of damage in Ge(HP) detectors may contain several stages, and its explanation is derived from other radiation damage literature. The further degradation of resolution after cycling a lightly damaged device to 200° K is attributed to the break up of the large damage region into several smaller clusters with each maintaining a substantial steady state charge. Vacancies are not yet extremely mobile at 200° K but become so just above that temperature. Nearing room temperature, vacancies are found to be "expelled" by the damaged region, forming isolated defect complexes indicating that the clusters do dissolve at relatively low temperatures. Further annealing of all of the defects is apparently proven at or below 400-500° K in essential agreement with the experience of detector fabricators. Proton induced damage yielding smaller clusters or isolated defects anneals at a somewhat lower temperature-time schedule.

(7) The effect of the fast neutron energy spectrum on observable energy resolution degradation is not clear because few consistent data exist, and certainly more study is required. Fluences of higher energy neutrons (e.g., 16 MeV) are somewhat more effective than lower energy neutrons, but the factor which should be derived from measurements on identical detectors (or a single detector) is not well established. Further comments will be reserved for the conclusion of the last section which deals with defect production vs. neutron energy.

4. Energy Deposition by Fast Neutrons in Germanium

It is of interest to calculate in some detail the average energy transferred to a primary knock-on atom (PKA) and that portion which is available to cause displacements (vacancy interstitial pairs) in the germanium lattice for several relevant neutron energies. This calculation is commonplace and very sophisticated for silicon[32,33] and other important materials such as stainless steel[34-36] but apparently not available for germanium (except for[37]). It may not be clear how to relate the number of displacements per neutron to observable detector degradation, but adequate nuclear data exist so that a good start towards the understanding of the distribution of displacements within the germanium lattice can be made.

Germanium consists of five isotopes: ^{70}Ge (20.5 ± 3%), ^{72}Ge (27.3 ± 3%), ^{73}Ge (7.8%), ^{74}Ge (36.5 ± 3%), and ^{76}Ge (7.8%) which must all be considered. Some inspection of the cross sections indicated, however, that the two minor isotopes, ^{73}Ge and ^{76}Ge, generally followed the others, so for convenience they were

omitted in the detailed calculation with 70, 72, and 74 Ge considered to be the total.

The total cross section for natural germanium in the region of 5 MeV is ~ 4 b which yields a mean free path, $1/N\sigma_T$, of 5.6 cm. It is therefore appropriate to consider only single collisions per neutron for detectors of slightly lesser dimension.

The maximum energy which can be transferred in an elastic collision between an incident particle of mass M_1, and energy E_o, and a struck particle of mass M_2 is

$$E_{2max} = \frac{4M_1M_2}{(M_1+M_2)^2} E_o \equiv \alpha E_o \qquad (2)$$

If the probability for scattering is isotropic, the average energy transferred per collision (averaged over all angles) is just $E_{max}/2$. If, however, an angular distribution is to be found for the scatterings, the average energy transferred ($\bar{E}_R$ = average recoil energy) must be weighted according to the differential scattering cross section:

$$\bar{E}_R = \frac{1}{\sigma_T} \int E_R(\bar{\theta}') \frac{d\sigma(\bar{\theta}')}{d\Omega} \cdot d\Omega \qquad (3)$$

where, in this example the nomenclature indicates that $E_R(\bar{\theta}')$ and the differential scattering cross section are in the center of mass coordinates. Figure 10 shows the differential elastic cross section for the three Ge isotopes at 5 MeV which illustrates the pronounced forward scattering resulting in reduced energy transfer to the PKA. The similarity of the cross sections for each of the three isotopes is due to the optical model dependence on nuclear size, which varies very little over this small range of atomic weight. Because the neutron is very light compared to Ge, the center of mass coordinates and lab coordinates are nearly identical so that lab coordinates can be directly used. Thus;

$$\bar{E}_R = \frac{1}{\sigma_T} \int_0^{\pi} E_R(\bar{\theta}') \frac{d\sigma(\bar{\theta}')}{d\Omega} \cdot 2\pi \sin\bar{\theta} \, d\bar{\theta} \qquad (4)$$

The energy transferred to the recoil particle as a function of lab angle $\bar{\theta}$ is just

$$E_R(\bar{\theta}) = (1-K(\bar{\theta}))E_o \qquad (5)$$

where $k(\bar{\theta})$ is the kinematic scattering factor, (familiar from Rutherford Backscattering) the fraction of energy retained by the incident particle.

$$K(\bar{\theta}) = \frac{M_1\cos\bar{\theta} + (M_2^2-M_1^2\sin^2\bar{\theta})^{\frac{1}{2}}}{(M_1+M_2)}^2 \qquad (6)$$

Inelastic scattering can also occur in which the recoil nucleus is left in an excited state by the nuclear collision. The kinetic energy of the recoil is thus reduced by the energy of the excited level of the resultant nuclear state after the collision. Because many excited levels may participate in the interaction, the evaluation of the average recoil energy must include a summation over many participating low lying nuclear energy levels. This summation and subsequent weighting must be carried out for each of the three isotopes 70, 72, and 74. It is acknowledged[38] that inelastic scattering is most probably isotropic and at worst results in equal probabilities for equivalent forward and back angles so that the average energy transferred to the recoils, again, one half of the maximum. The evaluation of the average recoil energy is, therefore

$$\bar{E}_R(\text{inel}) = \frac{1}{\sigma_T} \sum_{j=1}^{3} n_j \sum_i \sigma(E_i)E_{Ri} \qquad (7)$$

where $E_{R_i} = \frac{\alpha}{2}(E_o - E_i)$ and E_i is the energy of the ith nuclear excited state, $\sigma(E_i)$ is the total cross section to excite that level. n_j is the relative atomic fraction for each of ^{70}Ge, ^{72}Ge, and ^{74}Ge. Early work on detector damage[2] apparently underestimated the importance of inelastic scattering as has been the case for silicon.[39]

As the integrals and summations emerge, one must add one more physical ingredient, the division between recoil energy which goes into ionizing collisions (electronic excitation) and collisions which cause displacements or "nuclear" collisions. Bohr[40] first separated these two basic types of collisions in the slowing down process. Lindhard and associates followed with a series of calculations and demonstrations of the stopping powers for each of these collisions.[41] Without going into detail, Fig. (11) from Schiott[42] illustrates the relative importance of electronic and nuclear stopping powers as a function of recoil energy or the dimensionless Lindhard energy parameter, ε, which is proportional to the recoil energy. The nuclear portion, dominant at lower ion energies, is derived from numerical calculation of interactions based on a screened Thomas-Fermi potential. The electronic stopping power is found to have a simple form equal to $k\varepsilon^{\frac{1}{2}}$ where k is a parameter that is calculable but which can also be derived from experiment. Excellent reviews of this subject may also be found in conference papers by Robinson[43] and Sattler.[44]

Ironically, it was the advent of germanium detectors which gave an early opportunity to measure the electronic stopping fraction of germanium ions in germanium by inelastic neutron scattering to the first excited state in ^{72}Ge.[45] The Lindhard theory was largely confirmed at recoil energies above 100 keV and a series of further papers[46] pushed confirmation to recoil energies down to 250 eV. Figure (12) shows the data for the energy lost to ionization (or collected charge in a germanium detector) over a representative germanium ion energy range between 1 and 100 keV. The electronic fraction can be seen to be well represented by the parameter $k = 0.15$, and the electronic energy lost is $0.15\ E_R^{1.17}$. The energy lost in nuclear collisions causing displacements $E_D(E_R) = E_R - 0.15\ E_R^{1.17}$ which may be used in the preceding equations in place of E to directly compute the average energy available to cause displacements. Thus

$$\bar{E}_D = \frac{1}{\sigma_T} \cdot 2\pi \int_0^{\pi} E_D(E_R)(1-K(\bar{E}))E_o \frac{d\sigma_{el}}{d\Omega} \sin\theta d\theta + \sum_{j=1}^{3} \left(\sum_i \sigma_{in}(E_i) E_D(E_i) \right)_j \quad (8)$$

The differential elastic scattering cross section above may also be summed over that of each of the three major Ge isotopes or simply averaged if they are similar.

The values for the elastic and inelastic cross sections to be used in Eq. (8) above have been completed from optical model parameters by the National Nuclear Data Center at Brookhaven National Laboratory. It is a pleasure to directly acknowledge within this paper as well as later the generous help of Gus Prince and Frances Scheffel at the Nuclear Data Center. Computations of $\bar{E}_D$ have been made at three incident neutron energies, 2, 5, and 16 MeV which are of interest because of relevance to both commonly occurring energies such as fission spectrum, D-D or PuBe and D-T reaction energies, respectively, and therefore the energies that have been used in various investigations of neutron damage.

The average energy available to produce displacements is shown in Table I for the three neutron energies mentioned including the division between elastic and inelastic scattering.

TABLE I

Neutron Energy (MeV)	Total Cross Section (barns)	σ_{el}-$\bar{E}_D$ (b-keV)	σ_{inel}-$\bar{E}_D$ (b-keV)	$\bar{E}_D$ (keV)
2	3.54	42.6	31.3	20.9
5	3.96	60.59	106.3	42.14
16	3.05	70.45	337.6	133.6

It is apparent that the fraction of energy distributed by inelastic scattering increases with increasing neutron energy. This occurs because elastic scattering becomes increasingly forward directed, and the average recoil energy decreases with increasing neutron energy. Also the inelastic cross section itself increases with neutron energy as more levels become available to participate in the inelastic events. Previous estimates[3] of the energy available to recoils did not give sufficient weight to the effect of inelastic scattering. However, the 16 MeV result may overemphasize inelastic scattering as the more highly energetic inelastic events will tend to be forward directed, imparting less energy to the recoil. Piercy[36] calculates that E_D (in that case E_L) is 20.8 keV for a 1 MeV neutron in Zr.

The average number of defects produced may be calculated from the average energy available for defect formation $\bar{E}_D$ and the average (or isotropic) energy required per defect, E, which is essentially a lattice binding energy. This parameter has had several values but seems to gravitate towards 25 ev. Kinchin and Pease[37] point out in an early very comprehensive review that for a lattice displacement to occur, the PKA must have an energy of at least 2E; otherwise a collision may occur, but only one (or no) atom will be displaced. Collisions involving atoms with $E_D < E < 2ED$ will result in a new (but indistinguishable) displaced atom and are called replacement collisions. Because the energies of PKA's here are > 100 keV, far from 25 ev, we need not consider the nuances of very low energy collisions.[38] Thus the average number of displacements, $\bar{\nu}$, is $\bar{\nu} = E_D/2E$. It should be noted that in the Kinchin-Pease description and other earlier works, ν is really $E_D/2E$ and was assumed to be valid up to a PKA energy of "E_i", a cutoff energy, above which all the energy loss by the PKA goes into ionization. These models were used prior to the comprehensive treatment of energy partition between ionizing and atomic collisions given by Lindhard.[41] The Lindhard theory has been used here to give directly the energy available to atomic collisions, E_D, so that no upper limit should be expected. This approach has been termed the Lindhard model[34] in the radiation damage literature which supports the results shown in Table I.

Before characterizing the defects introduced by $\bar{E}_D$ in Table I, it may be instructive to list the average recoil energy at each neutron energy and the range of a PKA. Table II shows these values:

TABLE II

E_o MeV	$\bar{E}_D$ (keV)	$\bar{\nu} = \frac{\bar{E}_D}{2E}$	$\bar{\nu}/N\sigma_T$ Def./n-cm^{-1}	$\bar{E}_R$ (keV)	$\bar{R}(\text{Å})$ *	$\bar{\nu}/\bar{R}$
2	20.9	417	66	29.5	222	1.88
5	42.1	843	146	61.3	390	2.16
16	133.6	2672	361	225.6	1160	2.30

*Ranges from Schiott[42]

From Table II we find there are a large number of displacements caused over the range of the recoil, which will in some way coalesce to form highly disordered region(s) or cluster(s) that are the accepted result of the PKA. The ultimate effect on energy resolution of germanium detectors will depend on the hole trapping caused by either (or in portion, both) isolated defects from the cascade of the physical extent and charge on the larger cluster which will more stably result from this closely spaced deluge of vacancy interstitials.

Table II illustrates two extremes for the damage dependence on neutron energy. First, if the trapping cross section were not greatly dependent on disordered region charge, the density of the "cylinder" containing the cascade of vacancy interstitial pairs might be a dominant parameter; very little energy dependence on the hole trap production might result as suggested by the last column, $\bar{\nu}/\bar{R}$. If, however, the "size" (e.g. the $\bar{R}$) or the number of defects per neutron is the dominant parameter, a neutron energy dependence of approximately a factor of about 5 is expected between 2 and 16 MeV as shown in the fourth column. As Darken[4] argues, the steady state charge Q_{ss} per disordered region is certainly a most important parameter in the trapping cross section for large disordered regions and must be given great weight. Noting the nearly constant defect density for each energy, one might expect a nearly constant recombination rate for each case and therefore a steady state charge nearly proportional to the number of defects in the disordered region. Therefore the fourth column of Table II probably better indicates the energy dependence for fast neutron damage. Figure (13) is included to show the

best data that may exist (but which is admittedly rather selective) for detectors chosen for higher attainable fields from the study of 1974.[10] At the 3 keV level, the 16 MeV detector had received 1.5×10^9 n/cm^2, the 5.5 MeV detectors $\sim 6 \times 10^9$ n/cm^2. The range of fluences is not far from the range suggested in Table II. Certainly the energy dependence of observable damage is a study that should be made in much greater detail.

To give a final perspective on the nature of the nature of the displacement cascade several results of Avilov and Lenchenko[49,50] are presented. Figure (14) shows a Monte Carlo calculation presumably projected on two dimensions of the vacancy interstitial distributions of PKA's of 30 and 50 keV. Happily, the ranges shown graphically agree with those of Table II.

It was noted[49] that the channeling acceptance angle is proportional to 1/E and therefore channeling may play a role. Figure (15) shows the same calculation with channeling, and we note a means to create a distribution of smaller clusters.

Guided by Fig. (13), the volume affected by a PKA might be $\sim \pi(50\text{Å})^2$, R which is the home of 7.7×10^4, 1.35×10^5, and 4.02×10^5 Ge atoms for the 2, 5, and 16 MeV R, respectively. Dividing the number of defects, ν, of Table II by these numbers one gets between .5 and .7% of the matrix atoms affected within this region. Extreme damage by heavy charged particles has been considered[51] in terms of a displacement "spike" in which each atom in the region of the PKA (or near the end of its range) is displaced. The spike concepts are perhaps more applicable to metals wherein vacancy and interstitial migration is enhanced by strain gradients. The result with a little vacancy migration is directly a void. This concept was extended and described in[52] to temperature or energy spikes in which an appreciation was given to the fact that a great deal of energy was injected into a small volume in a short time. Calculations indicated that rapid melting of the region could occur also resulting in an amorphous volume or even a void. Thompson and Walker[53] in studying heavy ion implants in Si at 50° K suggest that spike effects are not important for defect fractions $< 10^{-3}$, and that defect densities must rise to greater than a few per cent before damage or defect distributions should be described as "spikes". The disordered region considered by Thompson and Walker was a volume similar to the cylinder over the PKA range suggested above. It is therefore probably inappropriate to consider the disordered regions in fast neutron irradiated germanium in terms of spikes.

Acknowledgements

It is a pleasure to acknowledge the discussions and associations with all collaborators during the development of this subject: C. Chasman, K. W. Jones, W. Brandt, R. H. Pehl, and E. E. Haller. The gracious help of A. Prince and F. Scheffel of the National Nuclear Data Center was invaluable in providing the extensive data on cross sections with which the displacement energies were then easily calculated. L. Darken generously provided a preprint and several drafts of his work on defect charge states and was very helpful in several conversations about this recent development. In the same vein, G. S. Hubbard and E. E. Haller provided their results prior to publication which are gratefully acknowledged. R. H. Pehl has contributed many discussions in detail over the course of study of this problem which have been extremely helpful. C. L. Snead, Jr. provided helpful perspective on radiation damage.

References

1. C. Chasman, K. W. Jones, and R. A. Ristinen, Nucl. Instr. & Meth. 37 (1965) 1.

2. H. W. Kraner, C. Chasman, and K. W. Jones, Nucl. Instr. & Meth. 62 (1968) 173 and "Semiconductor Nuclear Particle Detectors and Circuits", Publication 1593, National Academy of Sciences, Washington, D. C. (1969).

3. F. S. Goulding and R. H. Pehl, IEEE Trans. Nucl. Sci., NS-19, No. 1 (1971) 91.

4. L. S. Darken, Jr., T. W. Raudorf, R. C. Trammell, R. H. Pehl, and J. H. Elliott, "Mechanism for Fast Neutron Damage of Ge(HP) Detectors", Submitted to Nucl. Instr. & Methods.

5. G. S. Hubbard and E. E. Haller, IEEE Trans. Nucl. Sci. (this volume) Feb. 1980.

6. S. Wagner, Ortec Inc. and P. Ryge, Princeton Gamma-Tech, personal communications.

7. "Gatlinburg Conference on Radiation Effects in Semiconductors", J. Appl. Phys. August (1959).

   "Proceedings of the International Conference on Semiconductor Physics", Prague, 1960 Academic Press, N. Y. (1961).

   "The Interaction of Radiation with Solids", R. Strumane, J. Nihoul, R. Gevers, and S. Amelinckx, eds., North Holland Publishing Co., Amsterdam (1964).

   "Radiation Damage in Semiconductors", Paris Royaumont, 1964, Academic Press, N. Y. (1965).

   "Lattice Defects in Semiconductors", R. R. Hasiguti, ed., Penn. State University Press (1967).

   "Radiation Effects in Semiconductors", F. L. Vook, ed., Plenum Press, N. Y. (1968).

   "Radiation Effects in Semiconductors", J. W. Corbett and G. D. Watkins, eds., Gordon Breach Science Publishers, N. Y. (1971).

   "Radiation Effects in Semiconductors", N. B. Urli and J. W. Corbett, eds., The Institute of Physics, Bristol and London (1977).

8. P. H. Stelson, A. K. Dickens, S. Raman, and R. C. Trammell, Nucl. Instr. & Meth. 98 (1972) 481.

9. J. Llacer and H. W. Kraner, Nucl. Instr. & Meth. 98 (1972) 467.

10. H. W. Kraner, R. H. Pehl, and E. E. Haller, IEEE Trans. Nucl. Sci. NS-22, No. 1 (1975) 149.

11. E. E. Haller, W. L. Hansen, and F. S. Goulding, IEEE Trans. Nucl. Sci. NS-19, No. 3 (1972) 271.

12. R. H. Pehl, L. S. Varnell, and A. E. Metzger, IEEE Trans. Nucl. Sci. NS-25, No. 1 (1978) 409.

13. R. H. Pehl, N. W. Madden, J. H. Elliott, T. W. Raudorf, R. C. Trammell, and L. S. Darken, IEEE Trans. Nucl. Sci. NS-26, No. 1 (1979) 321.

References (Cont'd).

14. R. H. Pehl, "Germanium Gamma Ray Detectors", Phys. Today 30 (1977) 50.

15. R. H. Pehl, L. S. Varnell, and R. H. Parker, Bull. Am. Phys. Soc. 23 (1978) 71.

16. R. H. Pehl, "Gamma Ray Spectroscopy in Astrophysics", NASA Technical Memorandum 79619, Aug. (1978) 473.

17. M. Martini, Ortec Inc., personal communications.

18. R. F. Konopleva, S. R. Novikov, E. E. Rubinova, and S. M. Ryvkin, "Radiation Damage in Semiconductors", Pg. 287, Academic Press, N. Y. (1965).

19. P. Ryge, Princeton Gamma-Tech, personal communications.

20. J. H. Crawford and J. W. Cleland, J. Appl. Phys. 30 (1959) 1204.

21. B. R. Gossick, J. Appl. Phys. 30 (1959) 1214.

22. J. R. Parsons, R. W. Balluffi, and J. S. Koehler, Appl. Phys. Lett. 1 (1962) 57.

23. F. L. Vook and R. W. Balluffi, Phys. Rev. 113 (1959) 62.

24. F. L. Vook, Phys. Rev. 125 (1962) 855.

25. F. L. Vook, "Radiation Effects in Semiconductors", Pg. 51, Academic Press, N. Y. (1965).

26. M. Bertolotti, "Radiation Effects in Semiconductors", Pg. 311, Plenum Press, N. Y. (1968).

27. R. F. Konopleva and A. A. Yuferev, Sov. Phys. Semicond. 7 (1974) 1393.

28. Yu. V. Martynenko, Rad. Effects 29 (1976) 129.

29. Yu. V. Martynenko, Rad. Effects 41 (1979) 7.

30. R. E. Whan, J. Appl. Phys. 37 (1966) 2435.

31. R. E. Whan, Phys. Rev. 140 (1965) A690.

32. W. R. Van Antwerp and J. E. Youngblood, IEEE Trans. Nucl. Sci. NS-24, No. 6 (1977) 2521.

33. J. E. Lohkamp and J. M. McKenzie, IEEE Trans. Nuc. Sci. NS-22, No. 6 (1975) 2319.

34. D. G. Doran, Nucl. Sci. & Eng. 49 (1972) 130.

35. D. M. Parkin and A. N. Goland, Rad. Effects 28 (1976) 31.

36. G. R. Piercy, J. Nucl. Mater. 29 (1969) 267.

37. E. A. Kramer-Ageev, in "Dosimetry and Radiation Protection", L. R. Kimel, ed. (in Russian), No. 9 Atomizdat, Moscow (1969).

38. J. C. Hopkins and D. M. Drake, Nucl. Sci. and Eng. 36 (1969) 275.

39. V. F. Kosmach, V. M. Kulakov, V. I. Ostroumov, and A. M. Petukhov, Sov. Phys. Semicond. 6 (1972) 364.

40. N. Bohr, Kgl. Danske Vedenskab Selskab, Mat-Fys. Medd. 18, No. 8 (1948).

41. J. Lindhard, V. Nielsen, M. Scharff, and P. V. Thomsen. Kgl. Danske Vedenskab Selskab, Mat-Fys. Medd. 33, No. 10 (1963).

42. H. E. Schiott, Kgl. Danske Vedenskab Selskab, Mat-Fys. Medd. 35, No. 9 (1966).

43. M. T. Robinson, "Proc. Nuclear Fusion Reactors Conf.", Pg. 364, British Nuclear Energy Society, Culham Laboratory (September 1969).

44. A. R. Sattler, "Radiation Effects in Semiconductors", F. L. Vook, ed., Plenum Press, N. Y. (1968).

45. C. Chasman, K. W. Jones, and R. A. Ristinen, Phys. Rev. Lett. 15 (1965) 245.

46. C. Chasman, K. W. Jones, and J. T. Sample, Phys. Rev. 154 (1967) 239.

C. Chasman, K. W. Jones, H. W. Kraner, and W. Brandt, Phys. Rev. Lett. 21 (1968) 1430.

K. W. Jones and H. W. Kraner, Phys. Rev. C4 (1971) 125.

K. W. Jones and H. W. Kraner, Phys. Rev. A11 (1975) 1347.

47. G. H. Kinchin and R. S. Pease, Rept. Prog. in Prog. in Phys. 18 (1955) 1.

48. K. Ohmae and B. Hida, J. of Nucl. Mat. 42 (1972) 86.

49. Yu. Z. Akilov and V. M. Lenchenko, Sov. Phys. Semicond. 8, (1974) 18.

50. V. M. Lenchenko and Yu. Z. Akilov, Sov. Phys. Semicond. 5 (1971) 349.

51. J. A. Brinkman, Am. J. Phys. 24 (1956) 246.

52. G. J. Dienes and G. H. Vineyard, "Radiation Effects in Solids", Interscience Publishers, New York (1957).

53. D. A. Thompson and R. S. Walker, Rad. Effects 36 (1978) 91.

Figure Captions

Fig. 1 Pulse height spectra for the Ge(Li) detector irradiated with 1.1 MeV neutrons at fluences of 1.2×10^{10} n/cm^2 and 1.2×10^{11} n/cm^2.

Fig. 2 Two parameter spectra showing the dependence of pulse height on carrier type. The pulse rise time is displayed on the far y axis and the energy spectra of ^{60}Co are shown on the x axes. The neutron energy of the irradiation was 5.75 MeV. The ^{60}Co source was collimated and directed towards the n+ contact (hole traversal) in the middle display and towards the p+ contact (electron traversal) in the bottom display.

Fig. 3 Capacitance as a function of bias voltage for detector 1098-4 at several neutron fluences as measured by the injected pulser method.

Fig. 4 Oscillograph of preamplifier output wave forms of the pulser for detector 284-1.2 at several low biases following irradiation by 3×10^{10} n/cm^2 of 5.5 MeV neutrons.

Fig. 5 Effects of fast neutron fluence on the energy resolution of the 1332 keV ^{60}Co line for both conventional (outer contact n+, p, p+) configuration and reverse electrode configuration (outer contact p+, n, n+) for Ge(HP) coaxial detectors. Electronic noise has not been subtracted.

Fig. 6 Resolution transients observed in p-type coaxial Ge(HP) detector P382 and n-type coaxial detector N382 after cycling applied bias off to on. Both detectors had received fluences of fast neutrons of $\sim 10^{10}$ n/cm^2 and reached a steady state energy resolution to which each transient approaches as $t \to \infty$.

Fig. 7 Electron micrographs of disordered regions in fast neutron irradiated n-type germanium.

Fig. 8 The development of the 620 cm^{-1} infrared absorption band with annealing of oxygen doped germanium irradiated by fast neutrons at -50° C.

Fig. 9 Annealing curves for the several infrared absorption bands in fast neutron and electron irradiated oxygen doped germanium. Of particular interest here is the development of the 620 cm^{-1} band in the neutron irradiated case compared with the electron irradiated case.

Fig. 10 The optical model calculations of the differential scattering cross sections for 5 MeV neutrons from ^{70}Ge, ^{72}Ge, and ^{74}Ge in the laboratory system.

Fig. 11 Nuclear and electronic stopping powers based on the Lindhard theory.

Fig. 12 Experimental verification of the Lindhard theory of energy loss by ionization for Ge ions in Ge as a function of ion energy. Germanium recoil ions are produced in a germanium detector by inelastic neutron scattering and their ionization energy loss is observed as summed with the discrete radiation from the excited state of the inelastic scattering.

Fig. 13 The energy resolution for four detectors from Ref. (10) as a function of neutron fluence. The fast neutron irradiations were carried out at 1.6, 5.5, and 16.4 MeV.

Fig. 14 Monte Carlo calculations of the distribution of vacancy interstitial pairs from 30 and 50 keV Ge ions in germanium by Akilov and Lanchencho[49].

Fig. 15 Monte Carlo calculations of the distribution of vacancy interstitial pairs from 30 and 50 keV Ge ions in germanium from Akilov and Lanchencho[49]. In this case, the effect of channeling is included in the calculation.

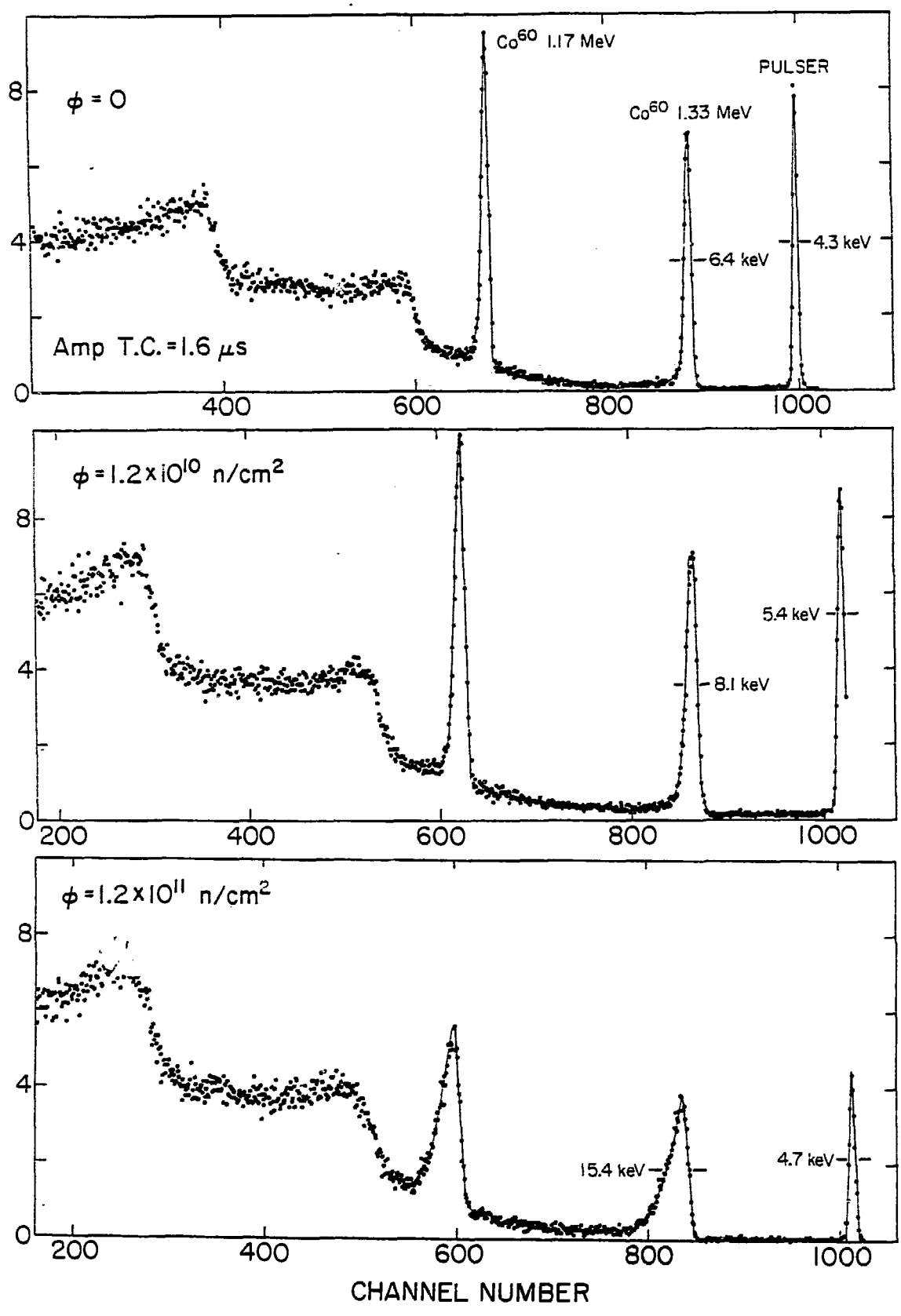
Co60 1.17 MeV
PULSER
Co60 1.33 MeV
φ = 0
6.4 keV
4.3 keV
Amp T.C. = 1.6 μs
φ = 1.2 x 10^10 n/cm^2
5.4 keV
8.1 keV
φ = 1.2 x 10^11 n/cm^2
15.4 keV
4.7 keV
CHANNEL NUMBER

FIGURE 1

DEPENDENCE OF PULSE HEIGHT ON TYPE OF CARRIER

$\bar{E}_n$ = 5.75 MeV

COLLIMATED Co^{60} GAMMA RAY SOURCE

ENERGY DISPERSION = 0.57 KeV/CHANNEL

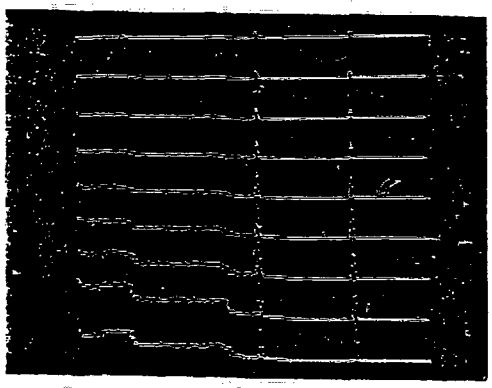

ϕ = 0 n/cm^2
GAMMA RAYS INCIDENT
NEAR p+ CONTACT

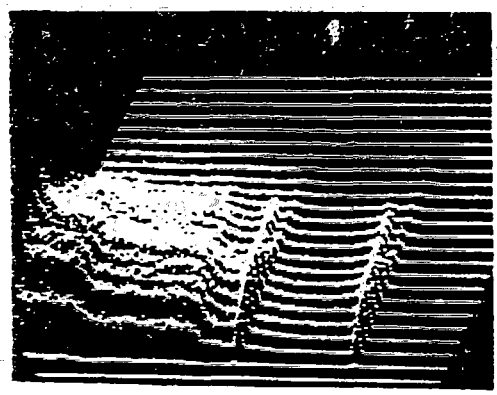

$\phi = 6.7 \times 10^{10}$ n/cm^2
GAMMA RAYS INCIDENT
NEAR n+ CONTACT

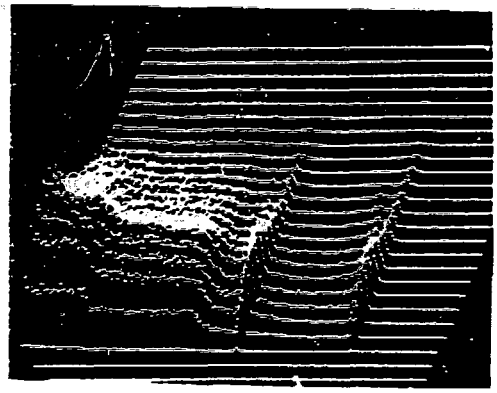

$\phi = 6.7 \times 10^{10}$ n/cm^2
GAMMA RAYS INCIDENT
NEAR p+ CONTACT

FIGURE 2

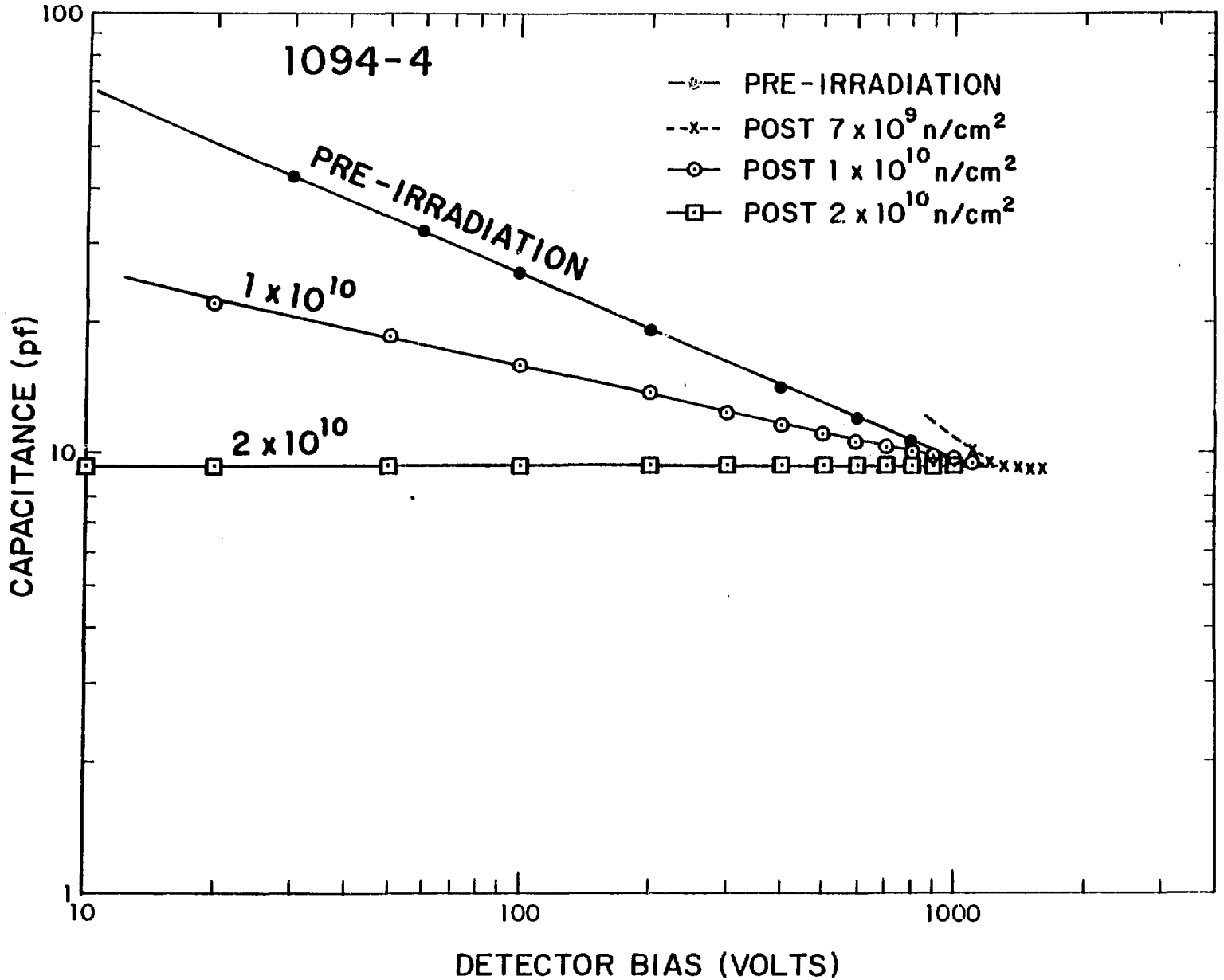
1094-4
PRE-IRRADIATION
POST 7 x 10^9 n/cm^2
POST 1 x 10^10 n/cm^2
POST 2 x 10^10 n/cm^2
PRE-IRRADIATION
1 x 10^10
2 x 10^10
CAPACITANCE (pf)
DETECTOR BIAS (VOLTS)
100
10
1
10
100
1000

FIGURE 3

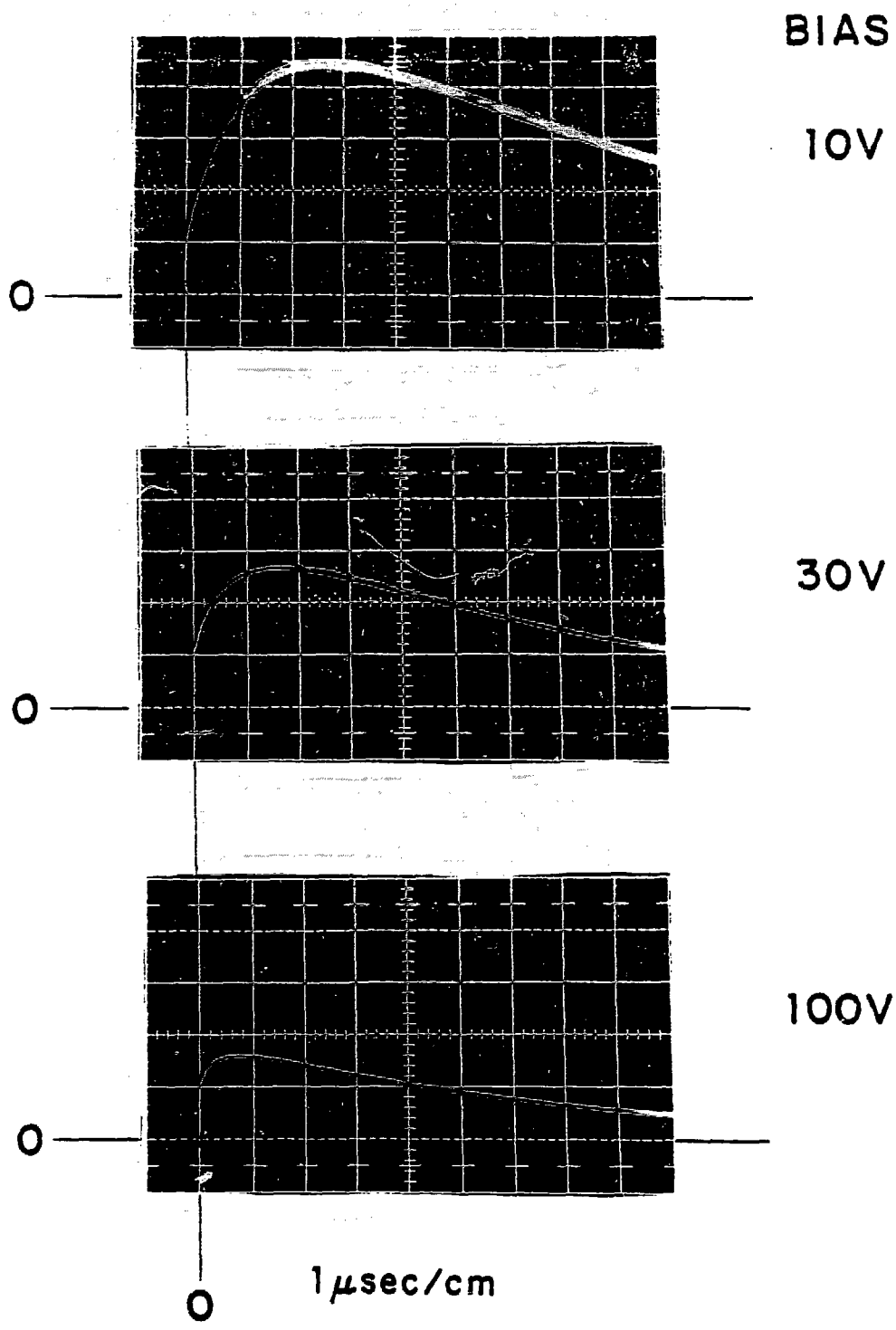

FIGURE 4

FIGURE 5

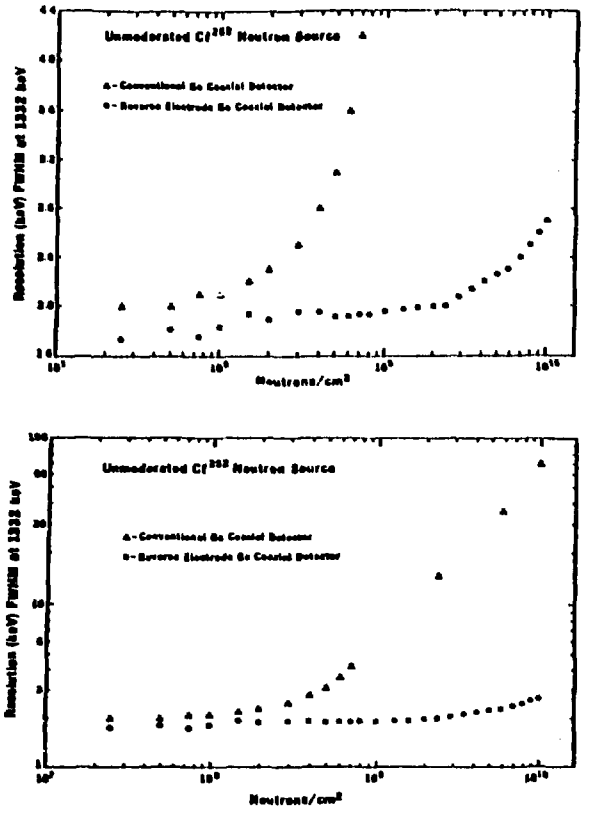

Fig. 3 Effect of neutron fluence on the energy resolution (FWHM) of the 1332 keV ^{60}Co line for both the conventional and reverse electrode configuration Ge coaxial detectors. Electronic noise has not been subtracted.

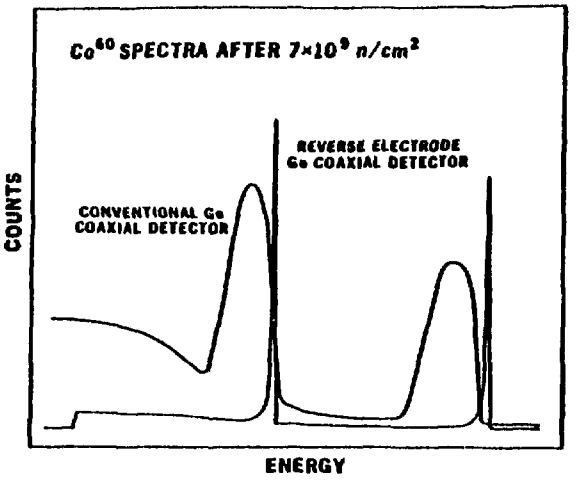

Fig. 4. ^{60}Co energy spectra obtained from both the conventional and reverse electrode configuration Ge coaxial detectors after a neutron fluence of 7×10^9 n/cm^2.

IEEE Transactions on Nuclear Science, Vol. NS-26, No. 1, February 1979

RADIATION DAMAGE RESISTANCE OF REVERSE ELECTRODE GE COAXIAL DETECTORS

Richard H. Pehl*, Norman W. Madden*, Jack H. Elliott**
Thomas W. Raudorf+, Rex C. Trammell+ and Lawrence S. Darken, Jr.+

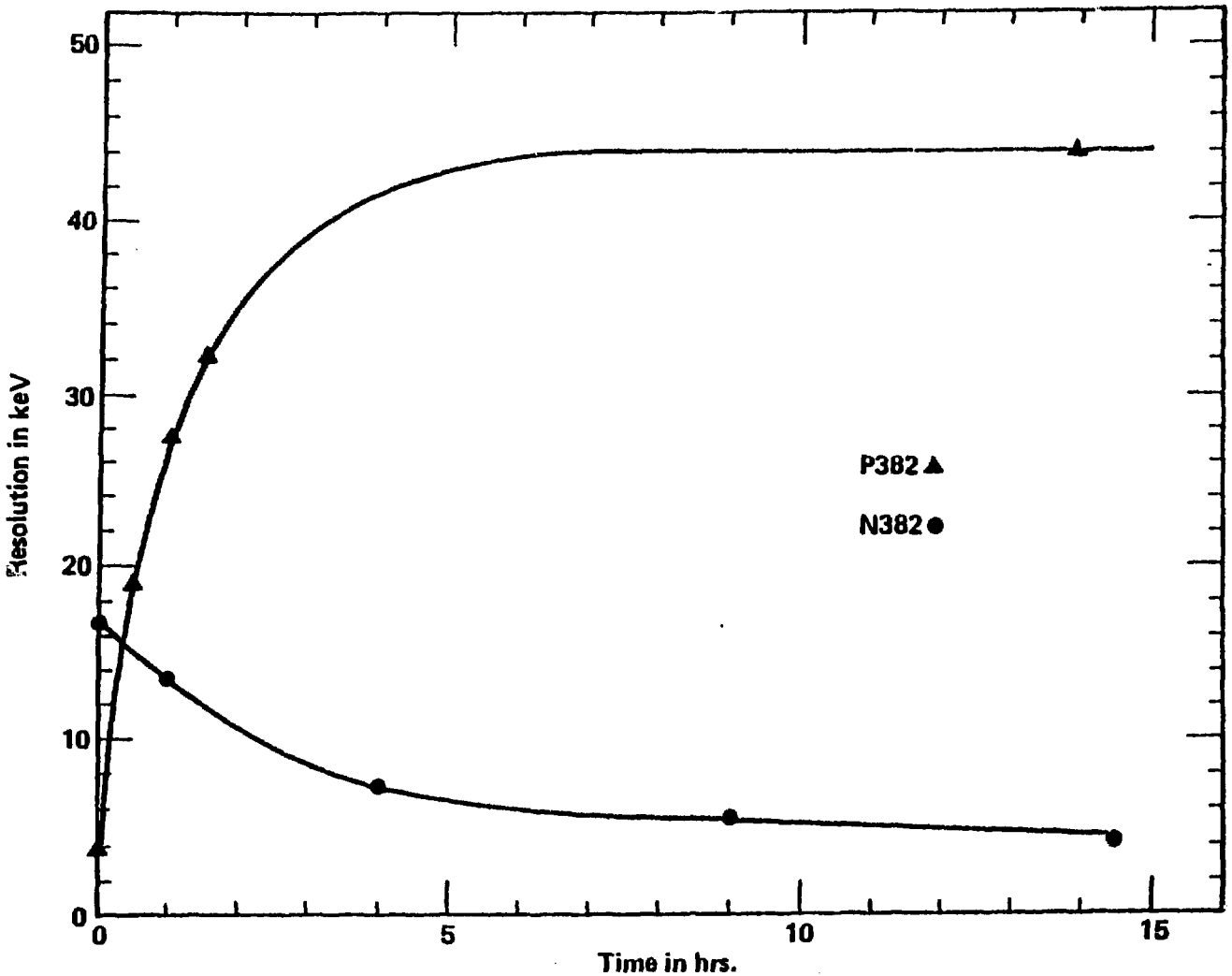

FIGURE 6

L. S. Darken, T. W. Raudorf, R. C. Trammell, R. H. Pehl and J. H. Elliott, "Mechanism for Fast Neutron Damage of Ge(HP) Detectors. Submitted to Nuclear Instruments and Methods.

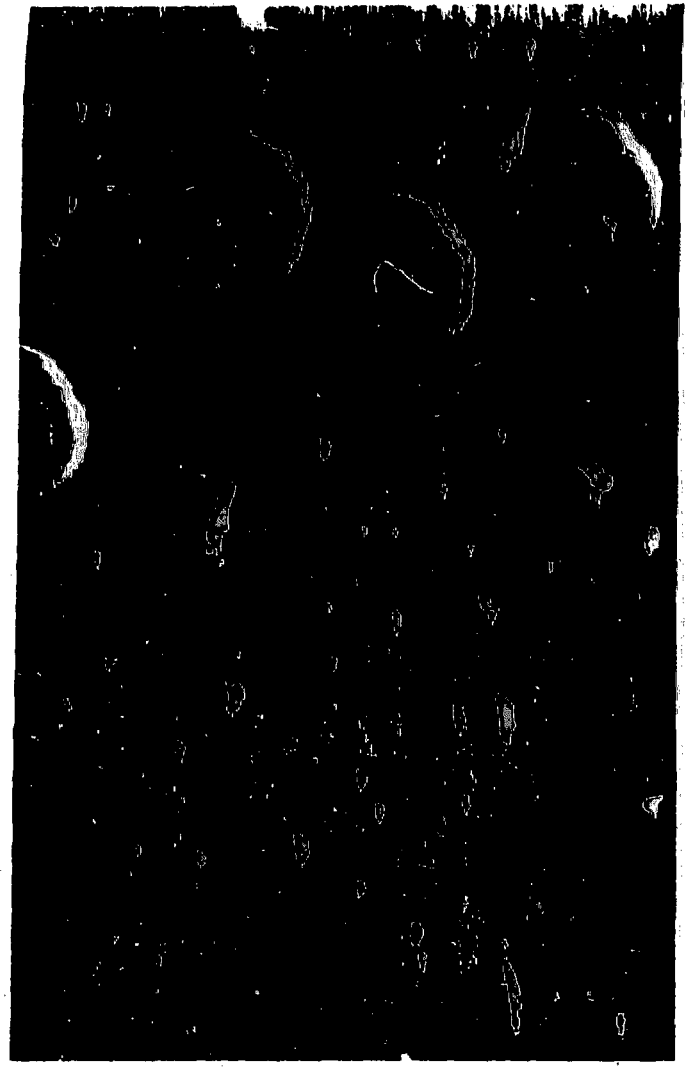

Fig. 1. General aspect of damage regions in neutron-irradiated n-type germanium

Fig. 2. Enlargement of a damage region in n-type germanium

region diameter 150-200 A

M. Bertolotti, Radiation Effects in Semiconductors, F. L. Vook, ed., Plenum Press, New York (1968).

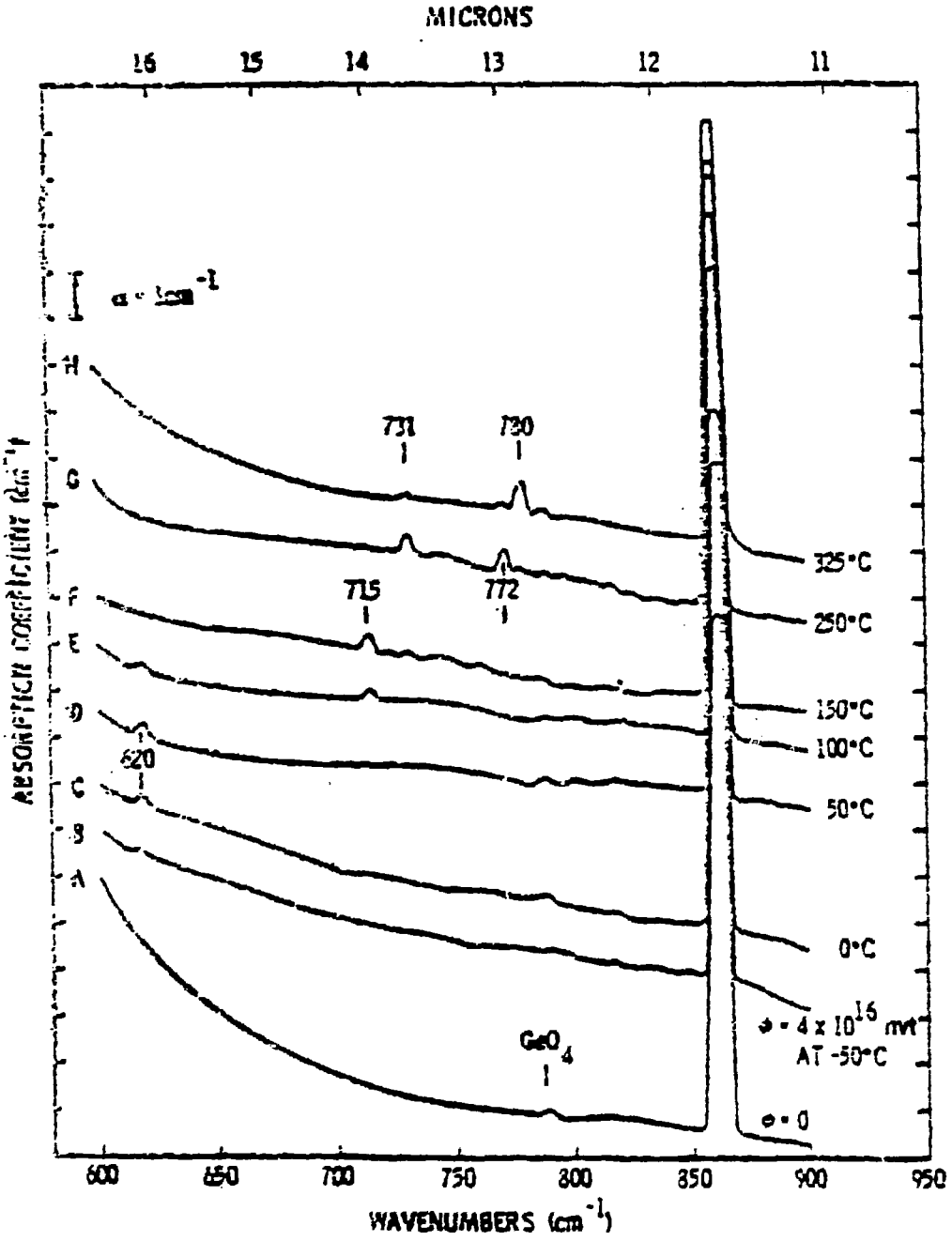

FIG. 3. Infrared absorption spectra of oxygen-doped germanium. All spectra recorded at 80°K. Spectra have been vertically displaced for clarity. A. $\Phi=0$, B. $\Phi=4\times10^{16}$ nvt>0.01 at -50°C. C. after 20-min anneal at 0°C, D. after 20-min anneal at 50°C, E. after 20-min anneal at 100°C, F. after 20-min anneal at 150°C. G. after 20-min anneal at 250°C, H. after 20-min anneal at 325°C.

R. E. Whan, J.O.A.P., 37, 2435 (1966).

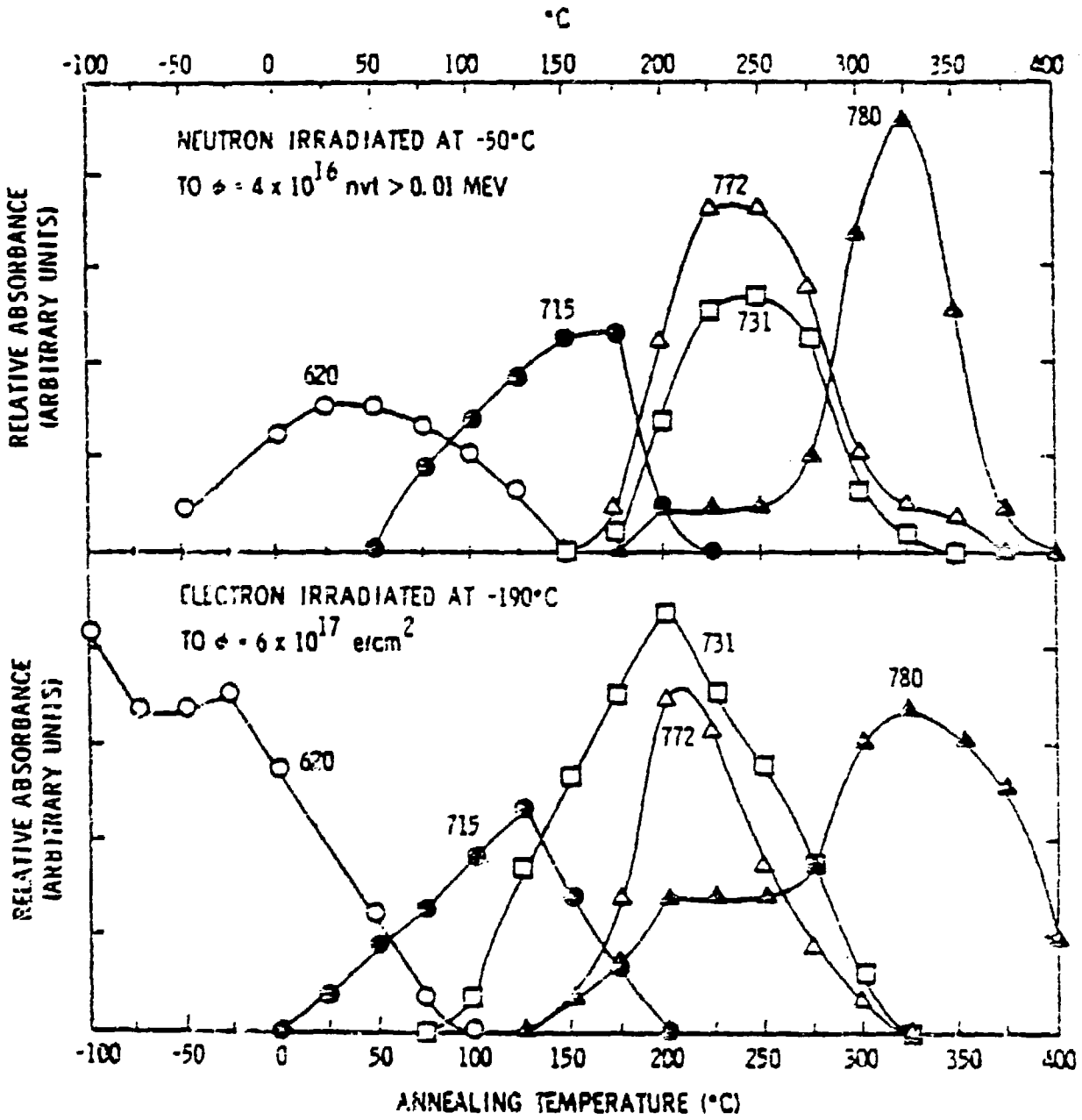

FIG. 4. Annealing curves for infrared absorption bands in the spectra of irradiated oxygen-doped germanium. Upper half—after neutron irradiation at $-50°C$ to $\Phi = 4 \times 10^{16}$ nvt > 0.01 MeV. Lower half—after 2-MeV electron irradiation at $-190°C$ to $\Phi = 6 \times 10^{17}$ electrons/cm^2.

R. E. Whan, J.O.A.P., 37, 2435 (1966).

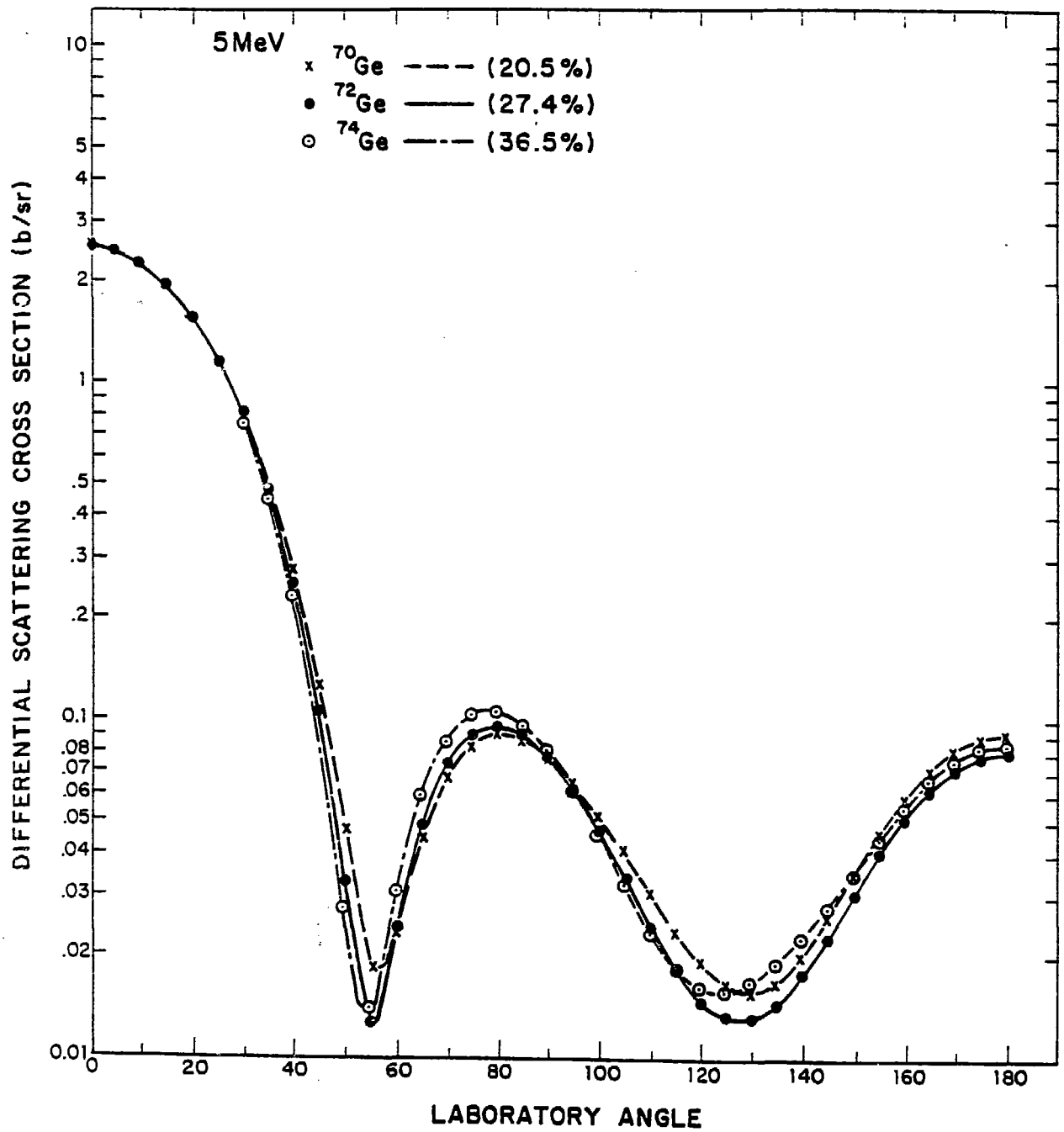
5MeV
^{70}Ge (20.5%)
^{72}Ge (27.4%)
^{74}Ge (36.5%)
DIFFERENTIAL SCATTERING CROSS SECTION (b/sr)
LABORATORY ANGLE
10
5
4
3
2
1
.5
.4
.3
.2
0.1
.08
.07
.06
.05
.04
.03
.02
0.01
0
20
40
60
80
100
120
140
160
180

FIGURE 10

FIGURE 11

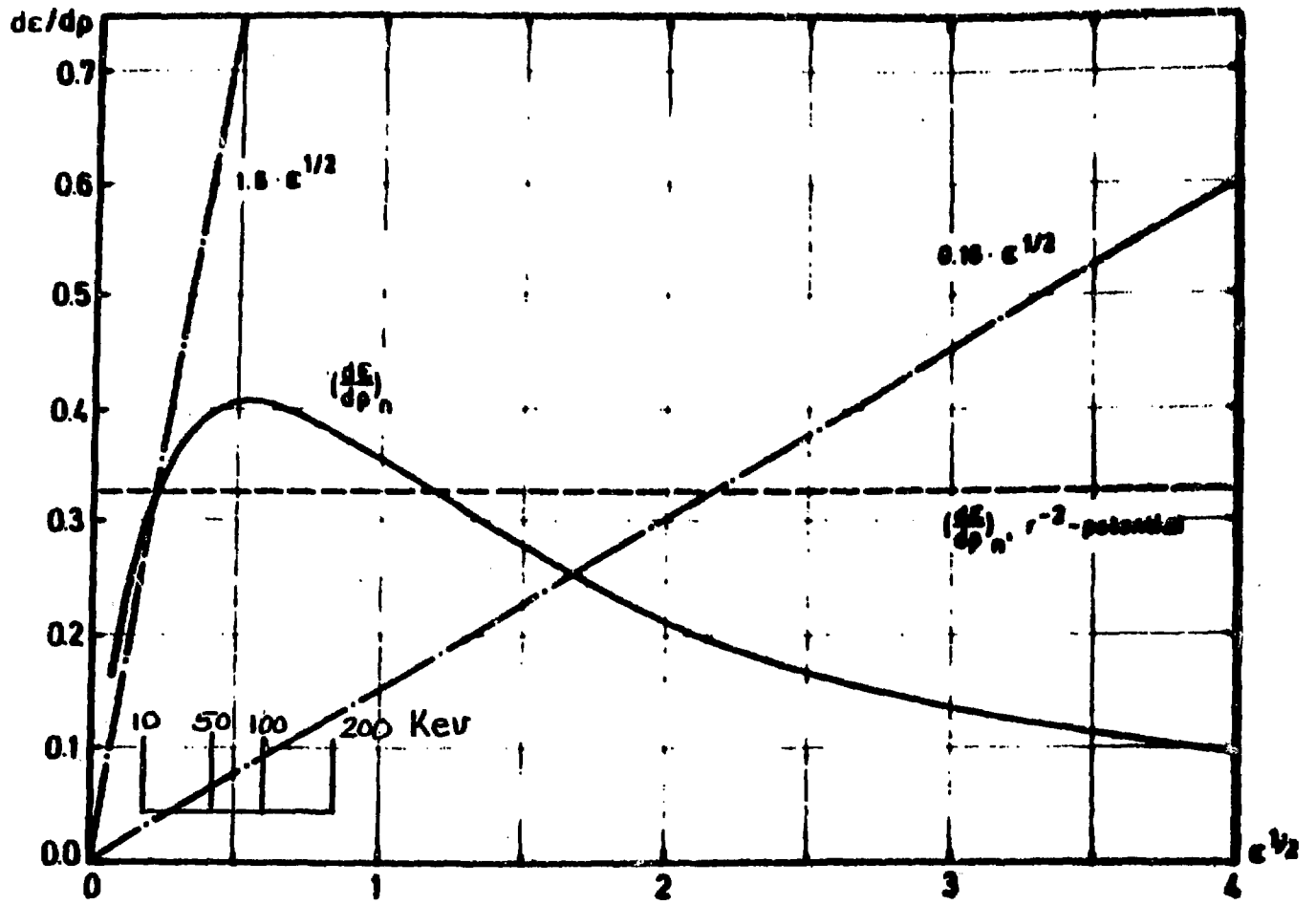

Figure 1. Nuclear and electronic stopping powers in reduced units. Full-drawn curve represents the Thomas-Fermi nuclear stopping power, the dot-and-dash lines the electronic stopping. (3), for k 0.15 and k = 1.5.

from: H. E. Schiott, Kgl. Danske Videnskab, Mat.-Fys. Medd. 35, No.9(1966)

Energies of interest for Ge ions in Ge are indicated.

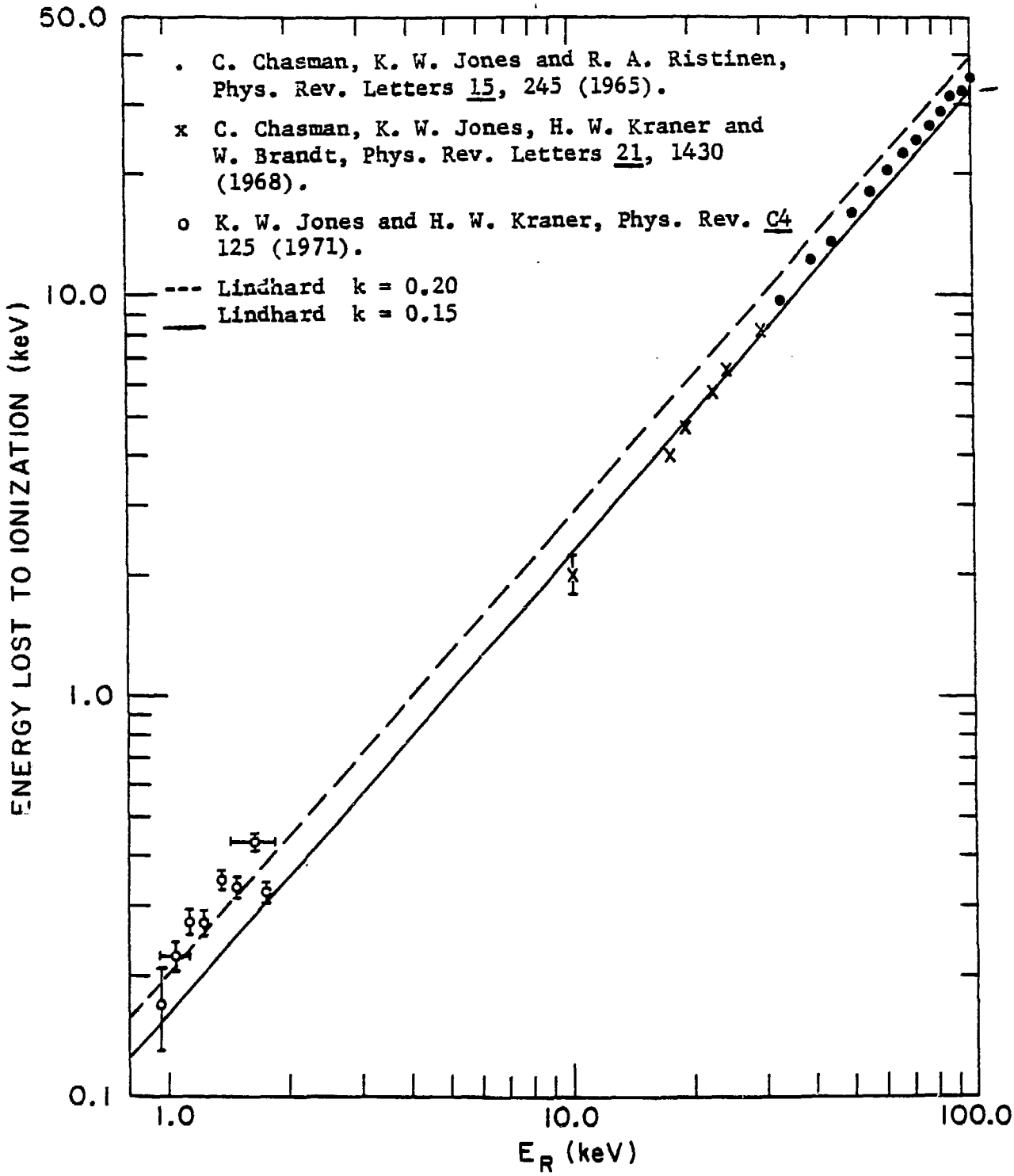
50.0
10.0
1.0
0.1
ENERGY LOST TO IONIZATION (keV)
. C. Chasman, K. W. Jones and R. A. Ristinen, Phys. Rev. Letters 15, 245 (1965).
x C. Chasman, K. W. Jones, H. W. Kraner and W. Brandt, Phys. Rev. Letters 21, 1430 (1968).
o K. W. Jones and H. W. Kraner, Phys. Rev. C4 125 (1971).
--- Lindhard k = 0.20
— Lindhard k = 0.15
1.0
10.0
100.0
E_R (keV)

FIGURE 12

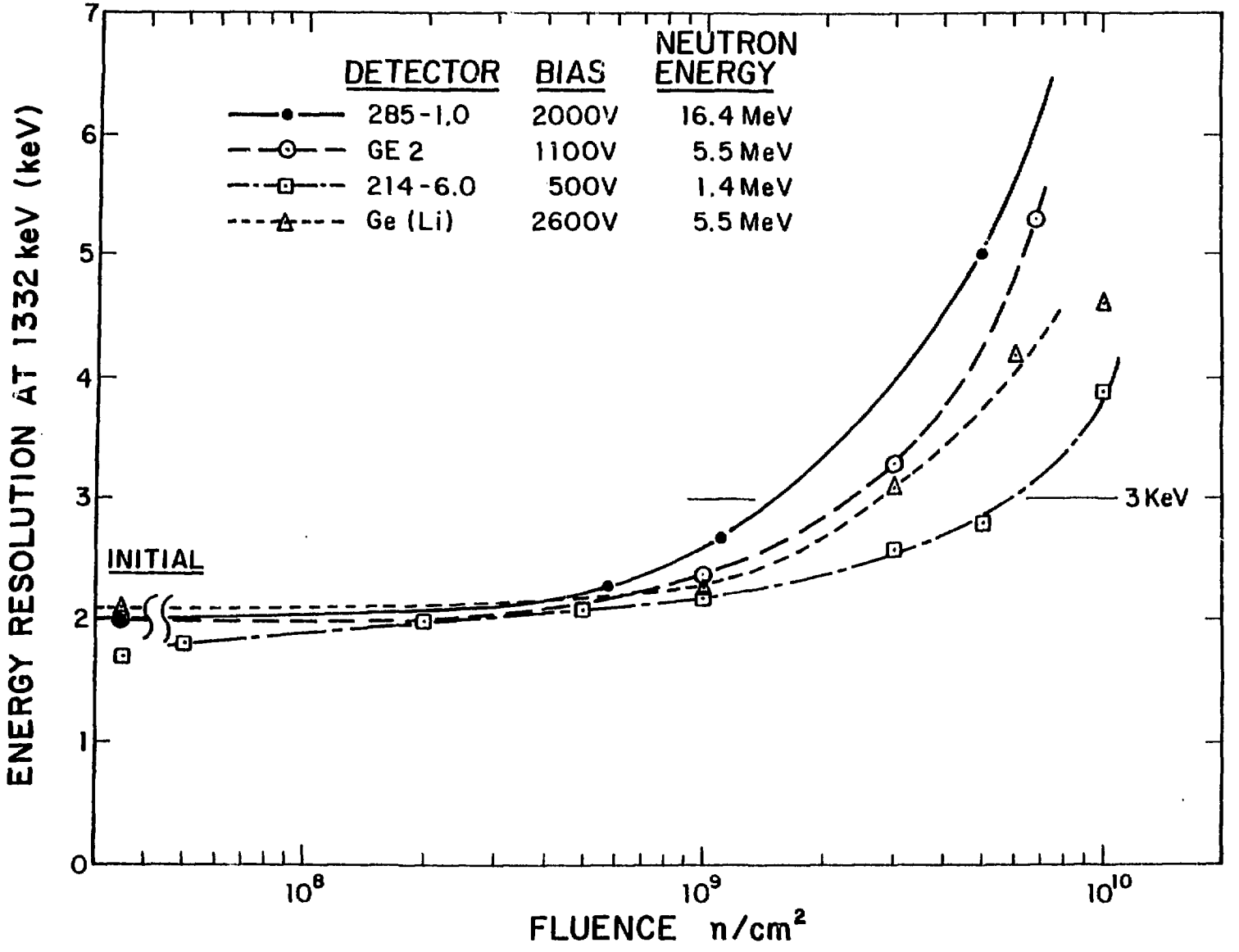
DETECTOR
BIAS
NEUTRON ENERGY
285-1.0 2000V 16.4 MeV
GE 2 1100V 5.5 MeV
214-6.0 500V 1.4 MeV
Ge (Li) 2600V 5.5 MeV
INITIAL
3 KeV
ENERGY RESOLUTION AT 1332 keV (keV)
FLUENCE n/cm²
0
1
2
3
4
5
6
7
10⁸
10⁹
10¹⁰

FIGURE 13

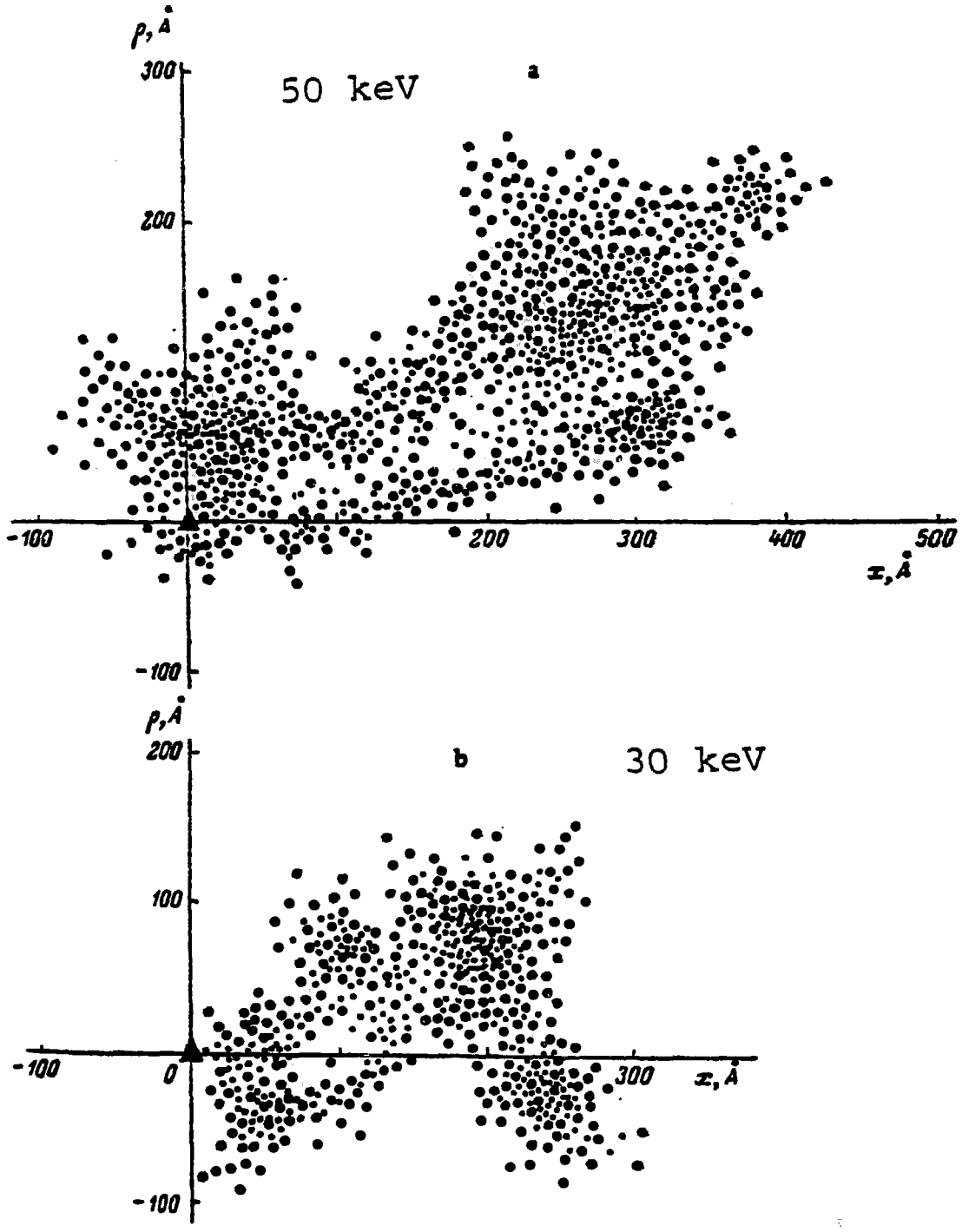

Fig. 2. Distribution of vacancies and interstitial atoms in Ge calculated by the Monte Carlo method.

Yu. Z. Akilov and V. M. Lenchenko, Sov. Phys. Semicond., 8, 18 (1974).

FIGURE 14

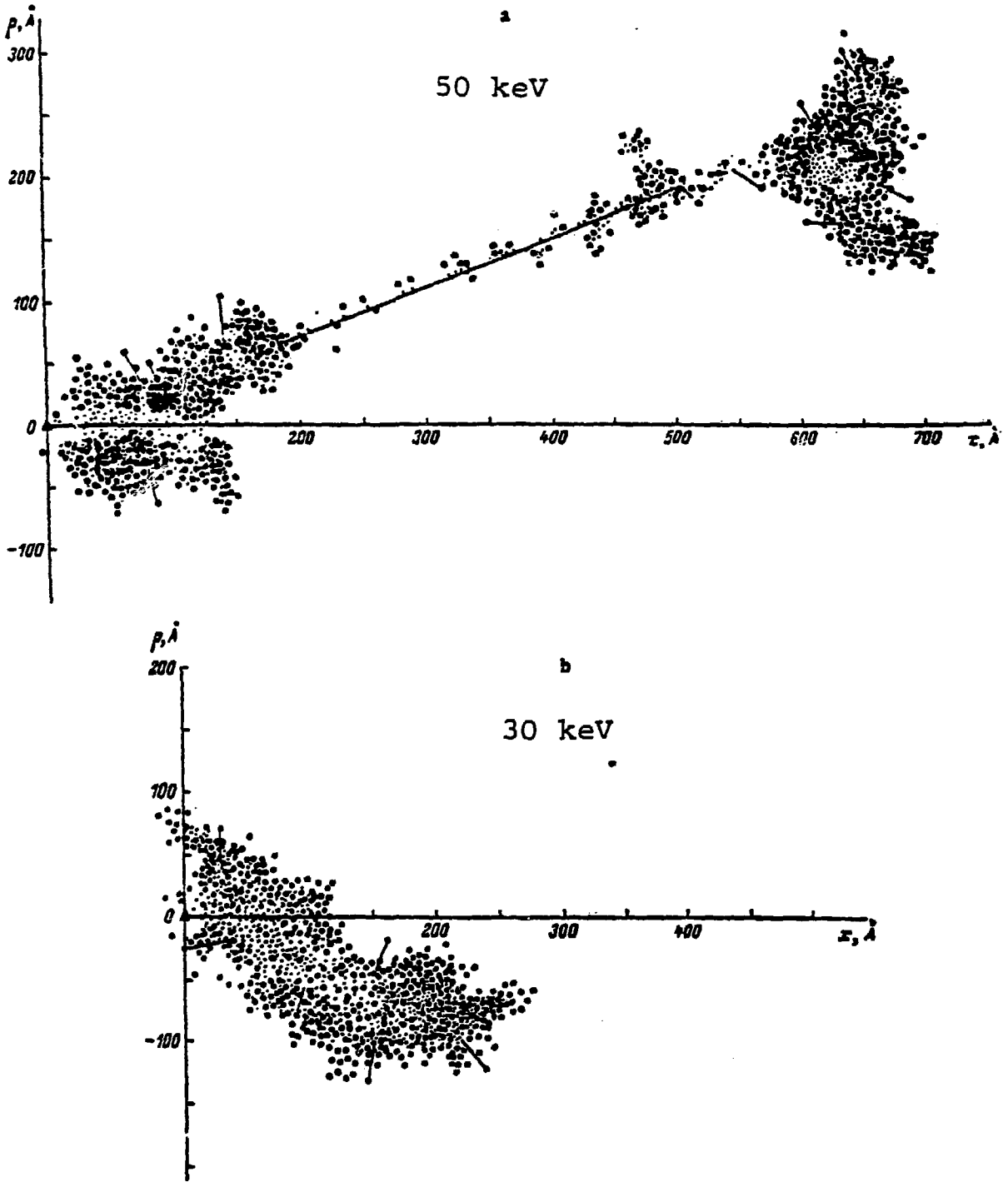

Fig. 4. Distribution of vacancies and interstitial atoms in a Ge single crystal. The short lines represent crowdions.

Yu. Z. Akilov and V. M. Lenchenko,
Sov. Phys. Semicond. 8, 18 (1974).